



# **Water Resources Research**

# **RESEARCH ARTICLE**

10.1029/2020WR028541

#### **Key Points:**

- Coupled sand-clay transport produced a low-conductivity layer beneath the zone of bedform scour
- Hyporheic exchange flux decreased linearly with kaolinite concentration in the bed
- Volume of porewater participating in hyporheic exchange decreased linearly at varying rates based on kaolinite pulse size

#### **Supporting Information:**

Supporting Information may be found in the online version of this article.

#### Correspondence to:

Y. Teitelbaum, teitelba@post.bgu.ac.il

#### Citation:

Teitelbaum, Y., Dallmann, J., Phillips, C. B., Packman, A. I., Schumer, R., Sund, N. L., et al. (2021). Dynamics of hyporheic exchange flux and fine particle deposition under moving bedforms. *Water Resources Research*, 57, e2020WR028541. https://doi.org/10.1029/2020WR028541

Received 3 AUG 2020 Accepted 11 MAR 2021

# Dynamics of Hyporheic Exchange Flux and Fine Particle Deposition Under Moving Bedforms

Yoni Teitelbaum<sup>1</sup>, Jonathan Dallmann<sup>2</sup>, Colin B. Phillips<sup>3,4</sup>, Aaron I. Packman<sup>3</sup>, Rina Schumer<sup>5</sup>, Nicole L. Sund<sup>5</sup>, Scott K. Hansen<sup>1</sup>, and Shai Arnon<sup>1</sup>

<sup>1</sup>Zuckerberg Institute for Water Research, The Jacob Blaustein Institutes for Desert Research, Ben-Gurion University of the Negev, Beersheba, Israel, <sup>2</sup>Department of Mechanical Engineering, Northwestern University, Evanston, IL, USA, <sup>3</sup>Department of Civil and Environmental Engineering, Northwestern University, Evanston, IL, USA, <sup>4</sup>Department of Civil and Environmental Engineering, Utah State University, Logan, UT, USA, <sup>5</sup>Desert Research Institute, Reno, NV, USA,

**Abstract** Deposition of fine suspended particles can reduce hyporheic exchange flux (HEF), which may result in impairment of various ecological processes. However, the dynamics of fine particle deposition and streambed clogging are still not well understood, especially when the bed is in motion. We conducted flume experiments to study the effects of coupled sand-clay dynamics on HEF with episodic (pulse) inputs of suspended kaolinite. Three experiments with a mobile sand bed and constant discharge were conducted with repeated injection of suspended kaolinite pulses at fixed concentration increments of 0.16, 0.41, and 0.66 g/L, respectively. HEF and participating porewater volume were assessed using tracer tests. Kaolinite deposition rates were inferred from turbidity measurements while deposition patterns were measured using core samples. We found that fine sediment primarily accumulated within a layer below the bedform scour zone, and that this layer was thicker when kaolinite was added in larger pulses. HEF declined linearly over time as kaolinite accumulated in the bed sediment; an increase of 0.1% kaolinite in the bed led to a decrease in HEF of 26.6 cm/day, regardless of the pulse concentration. However, the same kaolinite increase led to a reduction of 50% in participating pore volume for larger kaolinite pulses, versus only 30% for the smallest pulse. These results indicate that clogging occurs not just during and after high-flow events, but also under constant flow conditions in which episodic deposition of suspended clay by HEF leads to the formation of a low-conductivity layer in the bed.

## 1. Introduction

Rivers are a vital part of global ecosystems due to their major role in sediment distribution and cycling of nutrients and carbon (Cole et al., 2007; Tiegs et al., 2019). This is accomplished largely through the interactions between the flow in the stream and the underlying sediment bed. Interactions such as bed motion and water exchange between the stream and the subsurface are influenced by numerous physical properties including stream flow, streambed slope, particle size distribution of the bed, and so on. Biogeochemical processes in streams particularly depend on delivery of nutrients and substrates to microbes that are mostly found in the streambed (Battin et al., 2016; Boulton et al., 2010; Hester & Gooseff, 2010). Microbial metabolism is driven by exchange of surface water with the surrounding bed sediment (Boulton, 2007; Findlay, 1995; Trauth et al., 2015). Water that flows into the subsurface and returns to the stream after spending some time in the bed is referred to as hyporheic exchange (HE) and is vital for stream water quality (Boano et al., 2014; Cardenas, 2015; Harvey et al., 1996).

All streams and rivers carry fine suspended material that is composed of clay particles, organic matter, and microorganisms (Pachepsky & Shelton, 2011; Syvitski et al., 2003). These suspended particles interact with the bed through HE (Packman & Mackay, 2003) and thus particles in the water are deposited during flow into the bed (Partington et al., 2017). Over time or during events with high suspended matter concentrations in the water (e.g., during floods), fine suspended particle accumulation in the streambed can significantly alter the structure and the hydraulic characteristics of the bed. For example, accumulation of fine suspended particles in the streambed reduces the hydraulic conductivity ( $K_s$ ) and hyporheic exchange flux (HEF), and can divert flow paths (Fetzer et al., 2017; Fox et al., 2018; Packman & Mackay, 2003). These changes in particle dynamics and bed characteristics can occur naturally but have become more extreme in

© 2021. American Geophysical Union. All Rights Reserved.

TEITELBAUM ET AL. 1 of 13



recent decades as a result of increasing intensity of anthropogenic activity. Examples of such causes include surface erosion from agriculture, mining, urban development, landslides as a result of deforestation, and road-surface erosion (Nelson & Booth, 2002; Wolman, 1967; Wood & Armitage, 1997). Therefore there is a management imperative to understand the effects of changes to stream sediment budgets and alteration of fluvial habitat (Wharton et al., 2017; Wohl, 2015).

The amount of research devoted to understanding the phenomenon of particle deposition in streambeds has increased recently, especially with the increased awareness of the ecological impact of fine sediment accumulation in rivers. The study of the deposition dynamics of fine suspended particles in streambed sediment has been carried out using numerical models (Drummond et al., 2014; Karwan & Saiers, 2012; Packman et al., 2000a; Preziosi-Ribero et al., 2020), flume experiments (e.g., Fox et al., 2018; Gibson et al., 2009; Jin et al., 2019; Packman & Mackay, 2003; Rehg et al., 2005; Ren & Packman, 2002), and field studies (Brunke, 1999; Chen, 2004, 2011; Harvey et al., 2012; Karwan & Saiers, 2009; Phillips et al., 2019; Wu et al., 2015). Flume studies play a special role in understanding the processes involved in deposition of fine suspended particles in streambeds because they provide the ability to control the flow conditions, particle composition, water chemistry and streambed characteristics. Flume experiments also support direct measurements of streambed movement and structures (bedforms), which are formed by the coupling between surface water, boundary morphology, and bed sediment transport (Kennedy, 1969). Several flume studies have been carried out on kaolinite deposition and clogging, but mostly under low-flow velocities, below the critical shear for mobilization of the bed sediment, and with relict bedforms that originally formed under higher velocities (Fox et al., 2018; Jin et al., 2019; Packman et al., 2000b; Packman & Mackay, 2003). These studies show that hyporheic exchange and filtration causes kaolinite to deposit near the bed surface, leading to a reduction in HEF. However, stationary bedforms do not represent the prevalent situation in nature since most sand-bed rivers exhibit continuous sediment transport or frequent episodic motion.

Moving-bed conditions are more complicated than stationary beds because they introduce several feedback mechanisms. Flow into the bed carries particles through advection, or "pumping" (Elliott & Brooks, 1997). At the same time, moving bedforms exchange water and particles by trapping within the migrating streambed sediment and subsequent release due to erosion, a process known as "turnover" (Elliott & Brooks, 1997). Modeling studies have been carried out on the effect of bedform migration on porewater flow (Bottacin-Busolin & Marion, 2010), oxygen consumption (Ahmerkamp et al., 2015), and denitrification (Kessler et al., 2015; Zheng et al., 2019). Other studies have focused on measuring and modeling morphodynamic changes in streambeds under moving-bedform conditions (McElroy & Mohrig, 2009; Tonina et al., 2014; Voepel et al., 2013). The effect of bedform migration on oxygen consumption has also been assessed experimentally (Precht et al., 2004; Wolke et al., 2020). To date, research on fine particle deposition has primarily focused on net rates of clay deposition from the stream water (Mooneyham & Strom, 2018; Packman & Brooks, 2001; Ren & Packman, 2002), while comparatively less emphasis has been placed on the spatial and temporal dynamics of clay in the streambed itself. Recently, Dallmann et al. (2020) showed that under moving bedforms, clay accumulates in a layer coincident with the most frequent (modal) bedform scour depth, and this deposition decreases HEF. This finding supports older observations of patterns of clay accumulation in moving sand beds (Rehg et al., 2005). However, interactions between HEF, bedforms, and fine particle deposition are highly dynamic, and the effects of episodic clay inputs on these coupled dynamics have never been addressed. Thus, the objective of this study was to understand and quantify the effects of episodic inputs of clay on the coupled long-term dynamics of HEF and fine particle deposition under moving-bed conditions.

## 2. Materials and Methods

# 2.1. Experimental Setup and Overview of Approach

In order to assess the impact of moving bedforms on clay deposition and HEF dynamics, experiments were performed in a recirculating flume of length 640 cm by width 29 cm (Figure 1). The flume was filled with homogeneous sand (porosity: 0.33, hydraulic conductivity  $K_s = 0.12$  cm/s, mean diameter 384  $\mu$ m) to a height of approximately 20 cm, and deionized water with ~200 mg/L of NaCl added (resulting electrical conductivity, EC = 425  $\mu$ S/cm  $\pm$  10%). Surface water depth was maintained at 12 cm above the sand bed, and water was recirculated at a velocity of 0.31 m/s using a centrifugal pump (3LSF 50-125/4.0, EBARA).

TEITELBAUM ET AL. 2 of 13

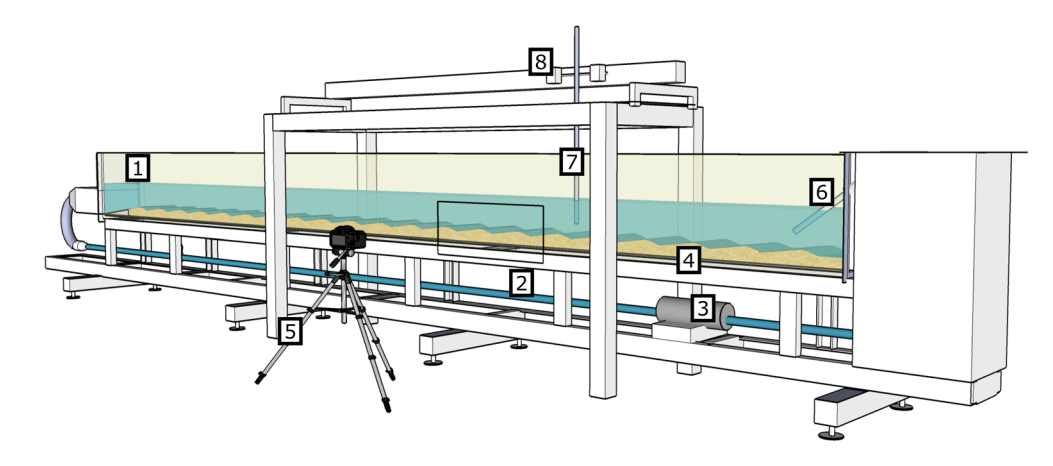


**Figure 1.** Schematic illustration of the flume used in the experiments. Main channel (1), circulation pipe (2), centrifugal pump for driving the flow in the channel (3), sand bed (4), tripod-mounted camera (5) for timelapse images through glass side wall of flume (black rectangle), mounted turbidity/EC sensors (6), acoustic/laser depth sensor (7) mounted on the Traverser system (8). Secondary loop and chilling system for regulating water temperature are not shown. Water flow is from left (inlet) to right (end well). EC, electrical conductivity.

Discharge in the channel was controlled by a 380V inverter (EDS1000 Series, ENC), and measured with a magnetic flow meter (Sitrans F M MAGFLO 5000, Siemens A/S). Water temperature was regulated by a chiller (Electra) in a secondary loop, with the water recirculated from the outlet of the flume using a centrifugal pump (NH-50 PX-Z, Pan World).

The three experiments each began with initial characterization of HEF using salt and dye tracer tests. Following the initial characterization, kaolinite clay (Agat Minerals Ltd., Text S1) was repeatedly added to the stream water. The mass of kaolinite was identical for all additions within a given experiment but varied between experiments. The number of kaolinite additions also varied from eight in the experiment with the smallest mass increment to four in the experiment with the largest one (Table 1). The number of additions per experiment was chosen due to a combination of factors. The upper-limit constraints were considerations of realistic water-column sediment concentration in sand-bed streams and measurement limits of our turbidity sensor, which cannot measure above 4000 NTU. At the same time, it is desirable to include as many additions as possible per experiment in order to assess the evolution of HEF and kaolinite deposition patterns over time. Within these constraints, the number of additions was chosen to achieve a similar range of bed sediment clay concentration in each experiment.

Clay concentration in the stream water was measured continuously with a turbidity meter (Visoturb IQ 700, WTW GmbH). The kaolinite additions led to suspended kaolinite concentrations of up to 1.4 g/L in the stream. These concentrations are well within the range that has been observed in the field (Blanchard et al., 2011; Kuhnle & Simon, 2000; Lenzi & Marchi, 2000; Loizeau & Dominik, 2000). HEF was measured using a salt tracer test 48 h after each kaolinite addition. At the end of each experiment, three analyses were conducted: HEF was measured using a salt tracer test and a dye penetration assessment, and the distribu-

tion of clay deposited in the bed was measured using core sampling. A detailed timeline of the different experiments is shown in Text S2.

**Table 1** *Kaolinite Additions in Each Experiment* 

Traction of Tractions of Europe States			
Experiment no.	Kaolinite mass in each clay addition (g)	Resulting increase in kaolinite free-stream concentration (g/L)	Number of additions
1	80	0.16	8
2	200	0.41	6
3	320	0.66	4

#### 2.2. Detailed Procedures and Measurement Methods

Kaolinite slurries were prepared by adding kaolinite (Table 1) to 5L solution of deionized water (DI) with 10 mM NaCl. The kaolinite was added gradually and stirred continuously during addition to prevent settling, and stirred for 24 h using a mechanical stirrer to enhance homogeneity. Following mixing, the kaolinite slurry was added to the flume. All mixtures were added to the flume by pouring them into the end well

TEITELBAUM ET AL. 3 of 13



(Figure 1) at a rate equal to the water recirculation time ( $\sim$ 60 s) to ensure thorough mixing with the flume water (Fox et al., 2018).

HEF was measured with salt tracer tests using an injection solution of 120g NaCl in 5L of flume water. After NaCl addition, surface water EC was recorded continuously every 30 s for 24 h using an EC sensor positioned in the surface water (Multi 3420 EC probe, WTW GmbH, Figure 1). Salt added to the surface water is diluted due to exchange with the pore water. Assuming that sediment porewater has an initial known and homogeneous EC, the change in EC over time can then be used to calculate the magnitude of the exchange flux using a mass balance (Fox et al., 2014; Packman et al., 2000b). The variability of this calculation was assessed during pre-experiment characterizations of the system and found to be  $\pm 5\%$ . The equilibrium EC at the end of this dilution indicates the volume of porewater that was exchanged with the water column (Text S3). Temporal rate of change of HEF as a function of kaolinite accumulation in the sediment bed was calculated using linear regression. Differences in decline of HEF and participating porewater volume between experiments were evaluated using analysis of covariance (ANCOVA).

The HEF values obtained from salt tracer tests were used to calculate  $K_s$  of the bed. This was accomplished with the following equation (Elliott & Brooks, 1997):

$$\overline{q} = \frac{K_s k h_m}{\pi} \tag{1}$$

where  $\overline{q}$  is HEF (m/s),  $K_s$  (m/s) is bed hydraulic conductivity, k is the bed wavenumber (1/m), and  $h_m$  (m) is the maximal head value along a bedform.

HE was also measured by dye tracing at the beginning and the end of each experiment. Brilliant Blue dye (25 g) was dissolved in 5L distilled water. Time lapse photographs were initiated just prior to addition of the dye and taken once per minute for 12 h to observe the propagation of the dye into the bed (Figure 1). These photographs were taken using a Nikon DSLR D5300 camera positioned perpendicularly to the glass sidewall of the flume, capturing dye distribution in the bed from the side along an 80-cm observation section of the flume. The percentage of bed sediment occupied by dye was computed using GNU Image Processing tool (GIMP) to measure dye penetration. Bed height was measured continuously using a Vectrino II Profiling Velocimeter (Nortek AS) mounted at a fixed location 5 m downstream of the flume inlet.

Turbidity was continuously measured using a turbidity sensor (Visoturb IQ 700, WTW GmbH) installed near the outlet of the flume (Figure 1) and the data were stored in a datalogger (HOBO U12-006, Onset Corp.) The amount of kaolinite deposited in the bed was calculated by monitoring decline in turbidity after each kaolinite addition, and by using a calibration curve between turbidity and kaolinite. Since sand and clay are efficiently recirculated within the flume system (no deposition of kaolinite or sand was observed in other parts of the system besides the sand bed), decline in water-column turbidity is considered to be indicative of kaolinite deposition in the bed. The amount of kaolinite in the bed was expressed as a percentage of bed sediment by dry mass (g/g). In order to assess the change in deposition patterns over time, the percentage of kaolinite deposited was calculated for each addition of kaolinite to the system. Each kaolinite addition cycle began with addition of kaolinite and then 48 h of waiting for the kaolinite to deposit before conducting a salt tracer test. The percentage of kaolinite deposited was calculated by taking the difference in surface water kaolinite concentration between the end and the beginning of the measurement period, divided by the mass of the kaolinite addition.

The amount of kaolinite deposited during the first 2 h after addition was also calculated. First the data were smoothed by fitting the data to a typical rate equation of the form

$$\frac{\mathrm{d}C}{\mathrm{d}t} = -\lambda C \tag{2}$$

where C (nondimensional) is relative surface water kaolinite concentration and  $\lambda$  (1/h) is the rate constant for kaolinite deposition. To improve the fit of the rate equation we allowed  $\lambda$  to vary linearly with clay deposited in the bed (i.e.,  $\lambda(C) = a0 + a1 \times (1 - C)$ ). All of the resulting fits had  $R^2 > 0.71$ . We also calculated the Rouse number (P) for insight on how the suspended kaolinite is transported in the water:

TEITELBAUM ET AL. 4 of 13

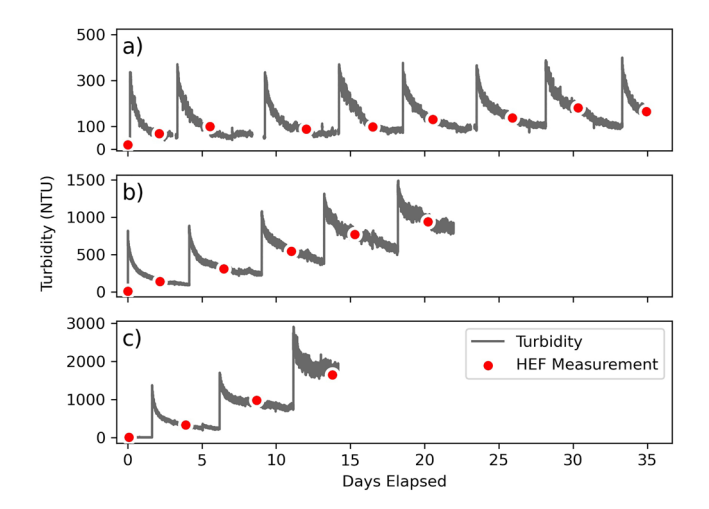


**Figure 2.** Water turbidity over time during each experiment: 0.16 g/L additions (a), 0.41 g/L additions (b), 0.66 g/L additions (c). Each spike in turbidity indicates a kaolinite addition. Red dots show the timing of HEF measurements. HEF, hyporheic exchange flux.

$$P = \frac{W_s}{\kappa u_*} \tag{3}$$

where  $W_s$  is the settling velocity of the suspended particle (m/s),  $\kappa$  is the von Karman constant (taken as 0.41), and  $u_*$  (m/s) is the shear velocity (calculated from the velocity profile using the log-law). Turbulent mixing and resuspension are considered to be dominant over gravitational settling when  $P \ll 1$  (Mooneyham & Strom, 2018). Bedform height was measured using the Vectrino profiler that was mounted at a fixed point along the flume, and sampled the elevation of the moving bed at a frequency of 2 Hz. Bedform height statistics for the moving bed were obtained from the series of bedforms that passed the profiler. The profiler data were analyzed within Python's SciPy package and consisted of acoustic depth measurements filtered with a second order Savitzky-Golay filter. Local maxima and minima in bed height (located with SciPy's "find\_peaks" function) indicate crests and troughs, respectively, of bedforms migrating downstream under the sensor. Bedform height was calculated as the difference in elevation between a trough and the subsequent crest. The minimum bedform height considered was 5 mm, and bed elevations smaller than this were filtered out of the data set. Bedform

length and celerity statistics were calculated from the aforementioned time lapse images as in Dallmann et al. (2020).

The spatial distribution of deposited kaolinite in the bed was measured at the end of each experiment by interpolating discrete kaolinite depth profiles beneath a topographic surface of the bed (Figure 1). The kaolinite accumulation profiles were measured through sediment cores subsampled at 0.5 cm depth increments. Thus each core resulted in a vertical stack of 10-15 measurements of kaolinite concentration. Surface relief of the bed was measured with a laser distance sensor (Model B0D 21M-LA02-S92, Balluff GmbH) mounted on a Traverser system (HR Wallingford). A 1.4-m-long, 18-cm-wide section was scanned at a 5 mm resolution a distance of 3.6-5 m from the inlet of the channel (Figure 1). This topographic relief of the bed was used to vertically align the cores with respect to each other. Afterward, 45 core samples were taken within the scanned section using 60-mL syringes with the ends cut off, following Fox et al. (2018) (Text S4). The cores were approximately 11 cm long with a diameter of 3 cm. All cores were sectioned into 0.5-cm-thick layers, and each core section was mixed with 30 mL of DI water and sonicated for 30 min to resuspend clay (Ultrasonic Cleaner Model ACP-300H, MRC Ltd.). The kaolinite concentration in the resulting suspension was measured using a spectrophotometer, at a wavelength of 480 nm. The water content of sand (wet mass) in each segment was also measured, and converted to a dry mass of sand using the average dry-to-wet mass ratio obtained from 20 segments. Five lengthwise concentration profiles at different points along the width of the flume were generated by linear interpolation between measured cores. These five profiles were then averaged to create a representative concentration profile for the entire bed.

# 3. Results

# 3.1. Surface Water Turbidity and Hyporheic Exchange

The kaolinite concentration of the surface water peaked immediately after each addition of kaolinite to the surface water, and then declined slowly as time progressed (Figure 2). Surface water kaolinite concentration did not decrease to background after any kaolinite addition, leading to an overall increase in the background concentration over the course of the experiments. The percentage of kaolinite that deposited in each addition was highest in the beginning of the experiment and generally decreased from one addition to the next (Text S5). The initial deposition rates varied both over the course of each experiment and between the three experiments (Figure 3a).

Initial deposition rates in all three experiments declined with increasing kaolinite accumulation, however there was a higher degree of variability between consecutive additions in the 0.16 g/L experiment

TEITELBAUM ET AL. 5 of 13

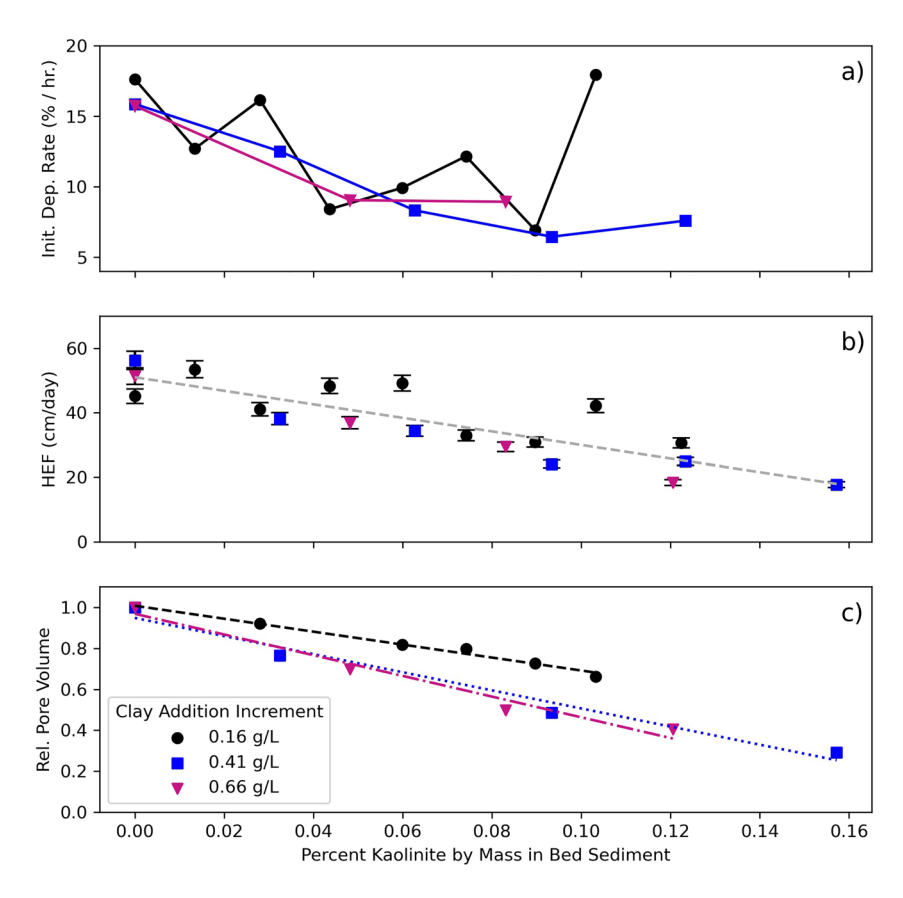


**Figure 3.** Initial deposition rates (a), decline of HEF during the kaolinite additions (b), and the relative pore volume participating in HEF (c) as a function of kaolinite deposited in the bed. Black circles, blue squares, and pink triangles represent 0.16, 0.41, and 0.66 g/L injection experiments, respectively. Error bars in (b) denote variability of  $\pm 5\%$  as determined during pre-experiment characterizations of the system. HEF, hyporheic exchange flux.

(Figure 3a). Specifically, for the two larger-increment experiments, initial deposition rate decreased monotonically, with the exception of the slight increase at the last addition of the 0.41 g/L experiment. Also for the two larger-increment experiments, the magnitude of change decreased monotonically from one addition to the next. For the 0.16 g/L experiment, meanwhile, neither the magnitude nor the direction of change between additions showed any predictable pattern.

HEF decreased gradually with increasing amount of kaolinite deposited in the bed in all three experiments (Figure 3b). HEF declined linearly as a function of clay accumulated in the bed. The slope of this decline was -141 (p < 0.05,  $R^2 = 0.84$ ), which implies that an increase of 0.1% kaolinite led to a decrease in HEF of 14.1 cm/day. There was no statistical difference between the rates of decline (ANCOVA, p > 0.05). However, there was comparatively more variability in the HEF measurements for the 0.16 g/L experiment ( $R^2 = 0.49$ , as compared to  $R^2 = 0.89$  and 0.996 for the 0.41 and 0.66 g/L experiments, respectively). Higher variability for the smallest injection concentration was also observed for the initial kaolinite deposition rate (Figure 3a). Note that there is one less data point per experiment in Figure 3a than in Figure 3b because the first measurement in Figure 3b is a baseline measurement, whereas the equivalent for kaolinite addition is simply the rate of deposition in the first addition. While kaolinite is still depositing during the HEF test, the HEF test is short in duration relative to the deposition period (less than half an hour, compared to 48 h of prior deposition) and occurs at a time when most of the kaolinite has already deposited (Text S3, Figure a). Therefore, it was assumed that HEF is static during the short time frame necessary for its calculation.

Pore volume participating in HEF also decreased as a function of kaolinite accumulated in the bed (Figure 3c). Unlike the HEF measurements, in this case there was a statistically significant difference between the 0.16 g/L experiment and the 0.66 g/L (ANCOVA, p < 0.05). No statistically significant difference was

TEITELBAUM ET AL. 6 of 13

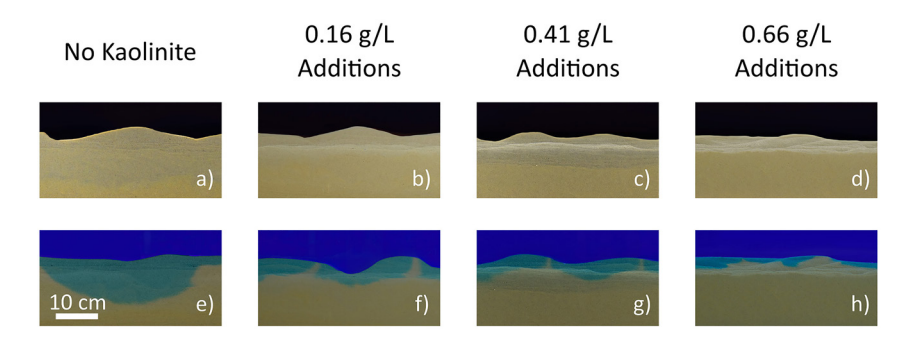


**Figure 4.** Photographs showing the streambed before dye addition (top row) and 3 h after dye was added (bottom row) for the clean sand bed (no kaolinite) and each kaolinite addition experiment. Images (b–d) and (f–h) were obtained at the end of their respective experiments, that is, after all kaolinite additions. Videos showing the temporal dynamics of the dye propagation in the bed are provided in Text S4.

found between the 0.41 and the 0.66 g/L experiments (ANCOVA, p > 0.05). The slope of the trend line for the 0.16 g/L experiment was -3.16, meaning that an increase of 0.1% kaolinite content implies a decrease of 0.316, or 31.6%, in the relative participating pore volume. The slopes for the 0.41 and 0.66 g/L experiments were -5.07 and -5.05, respectively. The decline in participating pore volume that was shown is also visible in photographs from dye additions (Figure 4). Kaolinite deposition impeded dye penetration with respect to the kaolinite-free bed in all three dye penetration tests (Figures 4e–4h). The degree of impediment increased with increasing kaolinite addition increment, as measured by the percentage of the bed sediment occupied by dye (29.68%, 24.37%, 17.93%, and 8.36% in Figures 4e–4h respectively).

# 3.2. Spatial Patterns of Kaolinite Deposition in the Bed and Bed Characteristics

Bed morphodynamics were continuously measured, and results are compared for the clean sand bed (before kaolinite addition) and after each kaolinite addition. The average and standard deviations of bedform heights, bedform length, and bedform celerity for the clean sand bed were  $1.7 \pm 0.7$  cm,  $35.88 \pm 26.51$  cm,  $8.79 \pm 3.85$  cm/hr, respectively. Bedform heights did not change over the course of any of the three experiments (Mann-Whitney U Test, p > 0.05). Celerity decreased by 9.8%, 53.8%, and 37.2% over the course of the 0.16, 0.41, and 0.66 g/L experiments, respectively. Change in bedform length was -34.5%, +13.0%, and +15.34% for the 0.16, 0.41, and 0.66 g/L experiments. Time lapse images showing the bed movement appear in Text S4.

Kaolinite deposition patterns varied between the three experiments. In the 0.16 g/L experiment, kaolinite accumulated in a thin layer several cm below the bed surface (Figures 4a and 4b). In the case of the 0.41 g/L additions, the kaolinite layer is somewhat thicker and more pronounced (Figure 4c). In the 0.66 g/L experiment, however, the kaolinite deposited throughout the upper few cm of the bed (Figure 4d). The qualitative patterns observed from the sidewall images (Figure 4) are also seen in the quantitative kaolinite concentration profiles obtained from core samples (Figure 5). In the 0.16 g/L experiment, kaolinite concentrations in the bed reached up to 0.96%, but the kaolinite in the scour zone was very low (Figure 5a). For the 0.41 g/L experiment, the kaolinite also deposited predominantly in a layer just below the scour zone, but had noticeably higher concentrations within the scour zone itself (Figure 5b) than for the 0.16 g/L experiment. However, the maximum local concentration for this experiment was 0.81%. Finally, at the end of the 0.66 g/L experiment, the kaolinite is present at the highest concentrations (up to 2.47%) throughout the scour zone (Figure 5c).

#### 4. Discussion

Previous studies have observed that suspended clay exchanges into porewater, deposits within the hyporheic zone, clogs the bed, and correspondingly decreases HEF (Packman & Mackay, 2003; Rehg et al., 2005). Here, we found that deposition rates generally decline as the kaolinite mass fraction in the bed increases, but the dynamics of this decline also depend on the mass of kaolinite introduced in each addition

TEITELBAUM ET AL. 7 of 13

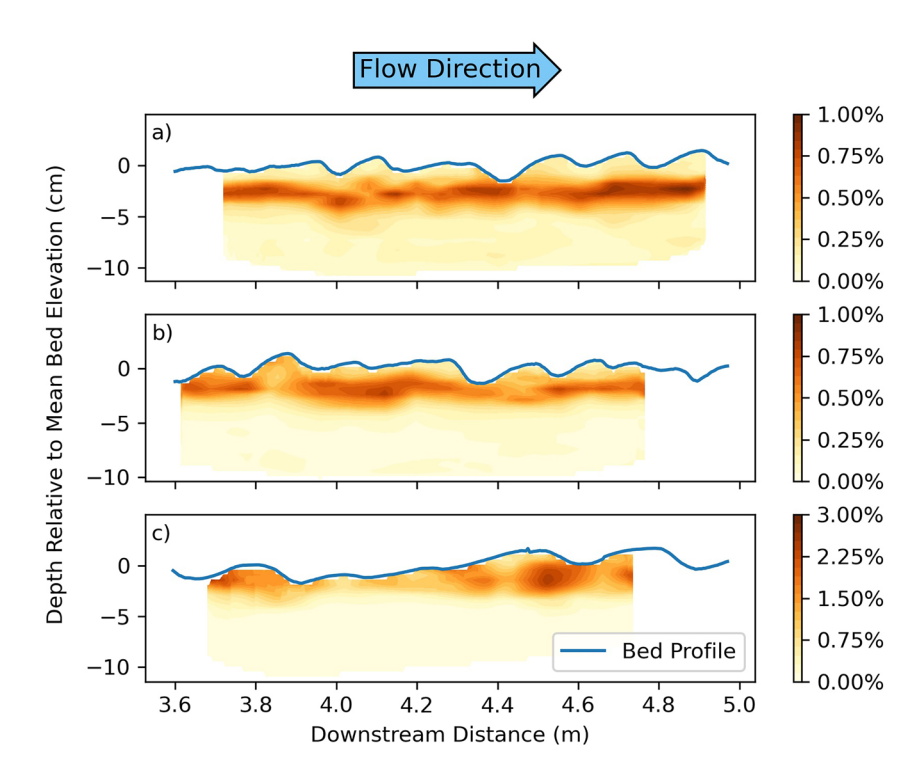


**Figure 5.** Kaolinite concentration in the sand bed at the end of the (a) 0.16 g/L experiment, (b) 0.41 g/L experiment, and (c) 0.66 g/L experiment. Note the different scale in (c). The blue line in each panel represents the bed surface profile, and the depth of 0 is the average bed height over the sampling area. The heatmap indicates the concentration of deposited clay obtained from interpolating data from multiple cores averaged across the width of the flume (see details in Section 2.2). Note that the concentration heatmap has a lower resolution than the bed surface profile, reflecting the resolution of the core samples.

(Figure 3a). These experiments reinforce previously observed fine particle deposition and remobilization dynamics (e.g., Dallmann et al., 2020; Rehg et al., 2005). Within the experiments conducted in this work, kaolinite was delivered into the bed by pumping-induced HEF and by mass transfer due to turbulence (Boano et al., 2014), where it is deposited via physicochemical filtration (Packman et al., 2000a). As the Stokes settling velocity of the kaolinite is approximately  $8.1 \times 10^{-4}$  m/s (Dallmann et al., 2020) and the Rouse number was 0.16, the conditions imply that all kaolinite remains in suspension (Rouse number <<1). Thus, we consider settling of kaolinite as playing a negligible role in bringing kaolinite into the bed from the water column compared to other mechanisms. Such observations were also made in other studies, which concluded that local conditions due to morphodynamics of the bed and local turbulence led to kaolinite deposition (Dallmann et al., 2020; Mooneyham & Strom, 2018; Phillips et al., 2019). However, settling may play a major role in transport of kaolinite within the bed sediment (Jin et al., 2019). Furthermore, under moving-bedform conditions the stream flow continuously remobilizes (scours) the top layer of sediment. This ongoing scour resuspends kaolinite that was deposited in that region of the bed, whereas kaolinite that deposited below the level of deepest scour remains in the bed. The result is vertical heterogeneity in kaolinite deposition. The accumulation of kaolinite in the bed sediment decreases porosity locally (Packman & Mackay, 2003). Where pore sizes decrease, kaolinite within advecting pore water is more likely to become trapped in the bed. Thus, following the next addition, kaolinite that reaches the depositional layer below the previous scour depth is more likely to deposit due to the increased filtration coefficient in that region (Fox et al., 2018). Following multiple additions, kaolinite accumulates in the region below the scour zone (Figures 4b, 4c and 5a). Similar behavior was observed by Dallmann et al. (2020) and Rehg et al. (2005) under different flow and morphodynamic conditions.

Scour depth has been observed to decrease with clay content in mixed sand-clay beds (Debnath & Chaudhuri, 2010; Molinas & Hosni, 1999). This implies that at a certain clay content and under certain shear conditions, scour depth will decrease (become shallower) and that the accumulated layer of kaolinite is

TEITELBAUM ET AL. 8 of 13



more likely to be preserved. As scour is a driving mechanism for resuspension of deposited kaolinite, a reduction in scour depth allows for greater accumulation of kaolinite at shallower depths, producing a cycle that continues until the whole upper layer of the bed is filled with kaolinite. This latter situation is a different vertically heterogeneous configuration: instead of a thin kaolinite layer separating two relatively kaolinite-free layers, there is just a single, thicker kaolinite-containing layer at the top of the bed. We suggest that the observed differences in thickness of the kaolinite layer and celerity are due to the increased bed stabilization under larger kaolinite addition increments. For larger clay additions, more kaolinite mass is deposited per addition. This is illustrated by the change in x-coordinate of successive points for each experiment in Figure 3b (the x-coordinate changes more between points for larger addition increments). More deposited kaolinite stabilizes the kaolinite layer at the bottom of the scour zone, protecting it from further scour (Dallmann et al., 2020), potentially increasing the filtration coefficient locally. When subsequent HEF delivers kaolinite into the bed at a later time, more kaolinite can accumulate due to the higher filtration coefficient, and a thicker kaolinite layer can form.

It is important to contextualize the increases in filtration coefficient and scour resistance that result from kaolinite accumulation. These increases are local phenomena, meaning that they only apply in the region where kaolinite accumulates. However, increased filtration coefficient and scour resistance at a given region of the bed do not necessarily imply an overall increase in the amount of kaolinite deposited in the bed, because that amount is also governed by the amount of kaolinite delivered into the bed by HEF. This results in a tradeoff between the competing processes that affect kaolinite deposition: increased retention of kaolinite due to increased filtration coefficient and increased scour resistance, and decreased delivery of kaolinite due to decreased HEF. These competing processes are not currently understood in enough detail to predict *a priori* which will dominate. In our experiments, we observed that HEF decreased over time in each experiment (Figures 3 and 4), and the overall amount of kaolinite deposited in the bed per addition decreased over time within each experiment as well (Text S5). We presume that the decrease in HEF caused the decrease in the amount of kaolinite deposited in the bed per addition. This means that the decrease in HEF dominated over the increase in filtration coefficient and resistance to scour in our experiments.

HEF decreased linearly with the amount of kaolinite in the bed, but the rate of decrease was not significantly different between the experiments (i.e., the rate of decrease did not change as a function of kaolinite addition increment). The reduction of HEF was caused by kaolinite deposition, which reduces streambed  $K_s$ (Fetzer et al., 2017; Fox et al., 2018; Packman & Mackay, 2003). In other words, kaolinite deposition created a layer of reduced  $K_s$  just below the scour zone (Figures 4e-4h). Streambed sediment deposits generally show complex patterns of lenticular structures formed by long-term sediment dynamics (Brunke, 1999; Chen, 2004, 2011; Wu et al., 2015). These patterns result in strong anisotropy in the near-surface permeability field (Chen, 2000, 2004). Even river channels that are primarily composed of sand have ratios of horizontal to vertical permeability of 10:1 or more (Chen, 2005). However, very few studies have assessed the effect of these structural arrangements on hyporheic exchange. Most studies to date have reported streambed clogging as a single  $K_s$  which provides one representative value for the bed, or as vertical and horizontal components ( $K_v$  and  $K_h$ , respectively) (Chen, 2000; Fox et al., 2016; Hatch et al., 2010; Song et al., 2007). Because of the preferential deposition of kaolinite in a horizontal layer below the scour zone it is expected that  $K_h$  will decrease less than  $K_v$  (Cheng et al., 2013). Indeed, the reduction in HEF during our experiments with moving bedforms was less than that reported for stationary bedforms, for which kaolinite deposits preferentially at locations of water-column inflow into the bed within bedforms (Fox et al., 2018; Jin et al., 2019; Rehg et al., 2005).

The overall  $K_s$  was reduced by over 50%. This reduction can be attributed primarily to the  $K_v$ , as evidenced by the combination of the linear declines in HEF and the participating pore water volume (Figures 3b and 3c). The linear rate of reduction in the volume of the participating porewater was lowest for the 0.16 g/L experiment, while no difference in the rate was seen for the higher concentration injection experiments (Figure 3c). By contrast, the decline in HEF occurred only as a function of clay deposited in the bed, and no statistically significant difference was found between experiments with different kaolinite mass additions. This apparent contradiction can be attributed to the fact that HEF measurements (Figure 3b) capture a shorter time frame (10–30 min after the addition) than the 24 h measurement period for the participating pore water (Figure 3c). Time lapse footage from dye penetration tests shows that over the period captured

TEITELBAUM ET AL. 9 of 13



by HEF measurements (Figure 3b), the tracer is still primarily constrained within the region of the bed above the kaolinite layer, while the time period captured within measurements of the pore water (Figure 3c) involves flow throughout the bed. Therefore the impact of the kaolinite layers is not apparent within the HEF measurements (Figure 3b), but can be seen in the participating porewater results due to the longer time window (Figure 3c).

There was much greater variability in both magnitude of HEF and initial deposition rate in the experiment with the lowest kaolinite mass (0.16 g/L) than in the other two experiments (Figures 3a and 3b). Initial deposition rate depends directly on HEF to deliver suspended kaolinite into the bed. Therefore, the fact that they both show this variability suggests that the variability is part of the system behavior and not due to measurement error. We attribute this behavior, along with slower decline of the participating pore volume for the 0.16 g/L experiment (Figure 3c), to the clay deposition-stabilization cycle. For the two larger kaolinite mass additions (0.41 and 0.66 g/L), kaolinite deposits quickly, making the bed more resistant to scour and thus leading to predictable decline in HEF over time. In the 0.16 g/L experiment, kaolinite does not deposit quickly enough to stabilize the bed, because less kaolinite is delivered into the bed per unit time due to lower water-column kaolinite concentration. As a result, the bed is much more susceptible to scour and resuspension of previously deposited kaolinite. Scoured sediment is replaced by sand that has been transported from upstream by saltation or in suspension, and upon redeposition this sand is essentially kaolinite-free. Thus periodic resuspension of sediment leads to the variability in HEF as observed in Figure 3a. The similarity of the two larger-increment experiments to each other in comparison to the 0.16 g/L experiment suggests that there is a threshold in kaolinite addition size above which the bed stabilizes. It appears that in cases where kaolinite deposits quickly enough to protect the bed from subsequent scour, the system displays consistent trends of decline of HEF with increased kaolinite in the bed.

Sediment deposition in rivers is traditionally seen as occurring under low-flow periods (via settling) and remobilization under high-flow periods (Partington et al., 2017). However, we demonstrate here that fine particle deposition occurs under flow velocities well above the conditions that are typically expected for significant settling of suspended matter, due to advective delivery of the fine particles into the streambed by hyporheic exchange flux. Moreover, we show that deposition and remobilization occur simultaneously due to bedform dynamics. The simultaneous deposition and resuspension of fine suspended particles under turbid conditions leads to a continuous, rather than sporadic, temporal pattern of clogging of the streambed.

The significant differences in clay depositional patterns observed here indicate that specific sampling efforts are required in order to adequately characterize the sediment structure and hydraulic characteristics of streambeds (Wharton et al., 2017). The role of sediment layering in reducing streambed  $K_s$  has been noted (Cheng et al., 2013; Freeze & Cherry, 1979; Pinder, 2011), and used to explain the temporal change in streambed  $K_s$  due to flow variations (Gianni et al., 2016; Korus et al., 2018; Wu et al., 2015). We show here that severe clogging can occur in a thin layer just below the base of the scour zone (i.e., within the top five cm of the bed in our experiments). While Korus et al. (2018) observed such thin low-conductivity layering, such small-scale structures are often overlooked in studies on streambed heterogeneity, which more commonly address the scale of tens of centimeters to meters. For example, Chen (2011), Song et al. (2007), and Korus et al. (2020) have demonstrated the anisotropy in  $K_s$  of sandy streambeds by measuring streambed sections of several tens of centimeters and concluded that clogging occurred due to larger-scale processes (e.g., deposition of low-conductivity layers after floods or mechanical rearrangement of the bed). Other studies found that hyporheic exchange explains deposition patterns of fine particles (e.g., Chen et al., 2013; Song et al., 2018), implying that the mechanism for clogging was simply advective transport and filtration. In this study, we found that these mechanisms combined with bedform scour to create heterogeneity in the sand bed in the form of a thin, laterally continuous region of high clay accumulation and low conductivity. The layered clay deposits and the resulting anisotropy that were observed in this study can be generated with substantial concentrations of wash load in the surface water, but can evolve differently over time depending on wash load concentration. Because even a thin low-conductivity layer can create strong anisotropy, and because the evolution of such a layer depends on the inherently transient phenomenon of wash load concentration, it is thus critical to obtain more detailed spatial and temporal measurements of streambed structure and  $K_s$  in order to understand the effect of water-column suspended clay content on HEF.

TEITELBAUM ET AL. 10 of 13



# **Data Availability Statement**

Data have been uploaded to the Hydroshare repository https://www.hydroshare.org/resource/7998bb-21207b41a3a036d58582bb59e4/ and will be made publicly available upon acceptance.

#### Acknowledgments

The authors thank Tomer Shimoni and Silvia Gobrecht for laboratory assistance. This research was supported by a grant from the US-Israel Binational Science Foundation (BSF), and the US National Science Foundation (NSF) (award number EAR-1734300) via the NSF-BSF joint program in Earth Sciences.

#### References

- Ahmerkamp, S., Winter, C., Janssen, F., Kuypers, M. M. M., & Holtappels, M. (2015). The impact of bedform migration on benthic oxygen fluxes. *Journal of Geophysical Research: Biogeosciences*, 1–14. https://doi.org/10.1002/2015JG003106
- Battin, T. J., Besemer, K., Bengtsson, M. M., Romani, A. M., & Packmann, A. I. (2016). The ecology and biogeochemistry of stream biofilms. Nature Reviews Microbiology, 14(4), 251–263. https://doi.org/10.1038/nrmicro.2016.15
- Blanchard, R. A., Ellison, C. A., Galloway, J. M., & Evans, D. A. (2011). Sediment concentrations, loads, and particle-size distributions in the Red River of the north and selected tributaries near Fargo, North Dakota, during the 2011 spring high-flow event (Scientific Investigations Report 5064): U.S. Geological Survey.
- Boano, F., Harvey, J. W., Marion, A., Packman, A. I., Revelli, R., Ridolfi, L., & Wörman, A. (2014). Hyporheic flow and transport processes: Mechanisms, models, and biogeochemical implications. *Reviews of Geophysics*, 52(4), 603–679. https://doi.org/10.1002/2012rg000417
- Bottacin-Busolin, A., & Marion, A. (2010). Combined role of advective pumping and mechanical dispersion on time scales of bed form-in-duced hyporheic exchange. Water Resources Research, 46(8), 1–12. https://doi.org/10.1029/2009wr008892
- Boulton, A. J. (2007). Hyporheic rehabilitation in rivers: Restoring vertical connectivity. Freshwater Biology, 52, 632–650. https://doi.org/10.1111/j.1365-2427.2006.01710.x
- Boulton, A. J., Datry, T., Kasahara, T., Mutz, M., & Stanford, J. A. (2010). Ecology and management of the hyporheic zone: Stream-ground-water interactions of running waters and their floodplains. *Journal of the North American Benthological Society*, 29(1), 26–40. https://doi.org/10.1899/08-017.1
- Brunke, M. (1999). Colmation and depth filtration within streambeds: Retention of particles in hypoheic interstices. *International Review of Hydrobiology*, 84(2), 99–117. https://doi.org/10.1002/iroh.199900014
- Cardenas, M. B. (2015). Hyporheic zone hydrologic science: A historical account of its emergence and a prospectus. Water Resources Research, 51, 3601–3616. https://doi.org/10.1002/2015wr017028
- Chen, X. (2000). Measurement of streambed hydraulic conductivity and its anisotropy. *Environmental Geology*, 39(12), 1317–1324. https://doi.org/10.1007/s002540000172
- Chen, X. (2004). Streambed hydraulic conductivity for rivers in South-Central Nebraska. *Journal of the American Water Resources Association*, 40(3), 561–573. https://doi.org/10.1111/j.1752-1688.2004.tb04443.x
- Chen, X. (2005). Statistical and geostatistical features of streambed hydraulic conductivities in the Platte River, Nebraska. *Environmental Geology*, 48(6), 693–701. https://doi.org/10.1007/s00254-005-0007-1
- Chen, X. (2011). Depth-dependent hydraulic conductivity distribution patterns of a streambed. *Hydrological Processes*, 25(2), 278–287. https://doi.org/10.1002/hyp.7844
- Chen, X., Dong, W., Ou, G., Wang, Z., & Liu, C. (2013). Gaining and losing stream reaches have opposite hydraulic conductivity distribution patterns. *Hydrology and Earth System Sciences*, 17, 2569–2579. https://doi.org/10.5194/hess-17-2569-2013
- Cheng, D.-h., Chen, X.-h., Huo, A.-d., Gao, M., & Wang, W.-k. (2013). Influence of bedding orientation on the anisotropy of hydraulic conductivity in a well-sorted fluvial sediment. *International Journal of Sediment Research*, 28(1), 118–125. https://doi.org/10.1016/s1001-6279(13)60024-4
- Cole, J. J., Prairie, Y. T., Caraco, N. F., McDowell, W. H., Tranvik, L. J., Striegl, R. G., et al. (2007). Plumbing the global carbon cycle: Integrating inland waters into the terrestrial carbon budget. *Ecosystems*, 10(1), 171–184. https://doi.org/10.1007/s10021-006-9013-8
- Dallmann, J., Phillips, C. B., Teitelbaum, Y., Sund, N., Schumer, R., Arnon, S., & Packman, A. I. (2020). Impacts of suspended clay particle deposition on sand-bed morphodynamics. Water Resources Research, 56(8). https://doi.org/10.1029/2019wr027010
- Debnath, K., & Chaudhuri, S. (2010). Laboratory experiments on local scour around cylinder for clay and clay-sand mixed beds. *Engineering Geology*, 111(1-4), 51-61. https://doi.org/10.1016/j.enggeo.2009.12.003
- Drummond, J. D., Aubeneau, A. F., & Packman, A. I. (2014). Stochastic modeling of fine particulate organic carbon dynamics in rivers. Water Resources Research, 50(5), 4341–4356. https://doi.org/10.1002/2013wr014665
- Elliott, A. H., & Brooks, N. H. (1997). Transfer of nonsorbing solutes to a streambed with bed forms: Theory. *Water Resources Research*, 33(1), 123–136. https://doi.org/10.1029/96wr02784
- Fetzer, J., Holzner, M., Plötze, M., & Furrer, G. (2017). Clogging of an Alpine streambed by silt-sized particles—Insights from laboratory and field experiments. Water Research, 126, 60–69. https://doi.org/10.1016/j.watres.2017.09.015
- Findlay, S. (1995). Importance of surface-subsurface exchange in stream ecosystems: The hyporheic zone. *Limnology & Oceanography*, 40(1), 159–164. https://doi.org/10.4319/lo.1995.40.1.0159
- Fox, A., Boano, F., & Arnon, S. (2014). Impact of losing and gaining streamflow conditions on hyporheic exchange fluxes induced by dune-shaped bed forms. Water Resources Research, 50(3). https://doi.org/10.1002/2013wr014668
- Fox, A., Laube, G., Schmidt, C., Fleckenstein, J. H., & Arnon, S. (2016). The effect of losing and gaining flow conditions on hyporheic exchange in heterogeneous streambeds. *Water Resources Research*, 52(9), 7460–7477. https://doi.org/10.1002/2016wr018677
- Fox, A., Packman, A. I., Boano, F., Phillips, C. B., & Arnon, S. (2018). Interactions between suspended kaolinite deposition and hyporheic exchange flux under losing and gaining flow conditions. *Geophysical Research Letters*, 45(9), 4077–4085. https://doi.org/10.1029/2018gl077951
- Freeze, R. A., & Cherry, J. (1979). Groundwater. Prentice-Hall.
- Gianni, G., Richon, J., Perrochet, P., Vogel, A., & Brunner, P. (2016). Rapid identification of transience in streambed conductance by inversion of floodwave responses. Water Resources Research, 52(4), 2647–2658. https://doi.org/10.1002/2015wr017154
- Gibson, S., Abraham, D., Heath, R., & Schoellhamer, D. (2009). Vertical gradational variability of fines deposited in a gravel framework. Sedimentology, 56(3), 661–676. https://doi.org/10.1111/j.1365-3091.2008.00991.x
- Harvey, J. W., Drummond, J. D., Martin, R. L., McPhillips, L. E., Packman, A. I., Jerolmack, D. J., et al. (2012). Hydrogeomorphology of the hyporheic zone: Stream solute and fine particle interactions with a dynamic streambed. *Journal of Geophysical Research*, 117(4), 1–20. https://doi.org/10.1029/2012jg002043

TEITELBAUM ET AL. 11 of 13



- Harvey, J. W., Wagner, B. J., & Bencala, K. E. (1996). Evaluating the reliability of the stream tracer approach to characterize stream-subsurface water exchange. Water Resources Research, 32(8), 2441–2451. https://doi.org/10.1029/96wr01268
- Hatch, C. E., Fisher, A. T., Ruehl, C. R., & Stemler, G. (2010). Spatial and temporal variations in streambed hydraulic conductivity quantified with time-series thermal methods. *Journal of Hydrology*, 389(3–4), 276–288. https://doi.org/10.1016/j.jhydrol.2010.05.046
- Hester, E. T., & Gooseff, M. N. (2010). Moving beyond the banks: Hyporheic restoration is fundamental to restoring ecological services and functions of streams. *Environmental Science & Technology*, 44(5), 1521–1525. https://doi.org/10.1021/es902988n
- Jin, G., Zhang, Z., Tang, H., Xiaoquan, Y., Li, L., & Barry, D. A. (2019). Colloid transport and distribution in the hyporheic zone. *Hydrological Processes*, 33, 932–944. https://doi.org/10.1002/hyp.13375
- Karwan, D. L., & Saiers, J. E. (2009). Influences of seasonal flow regime on the fate and transport of fine particles and a dissolved solute in a New England stream. Water Resources Research, 45(11), 1–9. https://doi.org/10.1029/2009wr008077
- Karwan, D. L., & Saiers, J. E. (2012). Hyporheic exchange and streambed filtration of suspended particles. Water Resources Research, 48, 1–12. https://doi.org/10.1029/2011wr011173
- Kennedy, J. F. (1969). The formation of sediment ripples, dunes, and antidunes. *Annual Review of Fluid Mechanics*, 1(1), 147–168. https://doi.org/10.1146/annurev.fl.01.010169.001051
- Kessler, A. J., Cardenas, M. B., & Cook, P. L. M. (2015). The negligible effect of bed form migration on denitrification in hyporheic zones of permeable sediments. *Journal of Geophysical Research: Biogeosciences*, 120, 1–11. https://doi.org/10.1002/2014JG002852
- Korus, J. T., Fraundorfer, W. P., Gilmore, T. E., & Karnik, K. (2020). Transient streambed hydraulic conductivity in channel and bar environments, Loup River, Nebraska. *Hydrological Processes*, (April), 3061–3077. https://doi.org/10.1002/hyp.13777
- Korus, J. T., Gilmore, T. E., Waszgis, M. M., & Mittelstet, A. R. (2018). Unit-bar migration and bar-trough deposition: Impacts on hydraulic conductivity and grain size heterogeneity in a sandy streambed. *Hydrogeology Journal*, 26(2), 553–564. https://doi.org/10.1007/s10040-017-1661-6
- Kuhnle, R., & Simon, A. (2000). Evaluation of sediment transport data for clean sediment TMDLs. USDA Agricultural Research Service. Lenzi, M. A., & Marchi, L. (2000). Suspended sediment load during floods in a small stream of the Dolomites (northeastern Italy). Catena, 39(4), 267–282. https://doi.org/10.1016/s0341-8162(00)00079-5
- Loizeau, J.-L., & Dominik, J. (2000). Evolution of the Upper Rhone River discharge and suspended sediment load during the last 80 years and some implications for Lake Geneva. *Aquatic Sciences*, 62(1), 54–67. https://doi.org/10.1007/s000270050075
- McElroy, B., & Mohrig, D. (2009). Nature of deformation of sandy bed forms. *Journal of Geophysical Research*, 114(3). https://doi.org/10.1029/2008jf001220
- Molinas, A., & Hosni, M. M. (1999). Effects of gradation and cohesion on bridge scour: Volume 4: Experimental study of scour around circular piers in cohesive soils (Vol. 4). US Department of Transportation, Federal Highway Administration.
- Mooneyham, C., & Strom, K. (2018). Deposition of suspended clay to open and sand-filled framework gravel beds in a laboratory flume. Water Resources Research, 54(1), 323–344. https://doi.org/10.1002/2017wr020748
- Nelson, E. J., & Booth, D. B. (2002). Sediment sources in an urbanizing, mixed land-use watershed. *Journal of Hydrology*, 264(1–4), 51–68. https://doi.org/10.1016/s0022-1694(02)00059-8
- Pachepsky, Y. A., & Shelton, D. R. (2011). Escherichia coliand fecal coliforms in freshwater and estuarine sediments. *Critical Reviews in Environmental Science and Technology*, 41(12), 1067–1110. https://doi.org/10.1080/10643380903392718
- Packman, A. I., & Brooks, N. H. (2001). Hyporheic exchange of solutes and colloids with moving bed forms. Water Resources Research, 37(10), 2591–2605. https://doi.org/10.1029/2001wr000477
- Packman, A. I., Brooks, N. H., & Morgan, J. J. (2000a). A physicochemical model for colloid exchange between a stream and a sand streambed with bed forms. Water Resources Research, 36(8), 2351–2361. https://doi.org/10.1029/2000wr900059
- Packman, A. I., Brooks, N. H., & Morgan, J. J. (2000b). Kaolinite exchange between a stream and streambed: Laboratory experiments and validation of a colloid transport model. Water Resources Research, 36(8), 2363–2372. https://doi.org/10.1029/2000wr900058
- Packman, A. I., & Mackay, J. S. (2003). Interplay of stream-subsurface exchange, clay particle deposition, and streambed evolution. Water Resources Research, 39(4), 1–10. https://doi.org/10.1029/2002wr001432
- Partington, D., Therrien, R., Simmons, C. T., & Brunner, P. (2017). Blueprint for a coupled model of sedimentology, hydrology, and hydrogeology in streambeds. *Reviews of Geophysics*, 55(2), 287–309. https://doi.org/10.1002/2016rg000530
- Phillips, C. B., Dallmann, J. D., Jerolmack, D. J., & Packman, A. I. (2019). Fine-particle deposition, retention, and resuspension within a sand-bedded stream are determined by streambed morphodynamics. *Water Resources Research*, 55(12), 303–318. https://doi.org/10.1029/2019wr025272
- Pinder, G. F. (2011). Groundwater hydrology: Groundwater quantity and quality management (2nd ed.). John Wiley and Sons. https://doi.org/10.1201/ebk1439815557-c9
- Precht, E., Franke, U., Polerecky, L., & Huettel, M. (2004). Oxygen dynamics in permeable sediments with wave-driven pore water exchange. Limnology & Oceanography, 49(3), 693–705. https://doi.org/10.4319/lo.2004.49.3.0693
- Preziosi-Ribero, A., Packman, A. I., Escobar-Vargas, J. A., Phillips, C. B., Donado, L. D., & Arnon, S. (2020). Fine sediment deposition and filtration under losing and gaining flow conditions: A particle tracking model approach. *Water Resources Research*, 56(2), 1–14. https://doi.org/10.1029/2019WR026057
- Rehg, K. J., Packman, A. I., & Ren, J. (2005). Effects of suspended sediment characteristics and bed sediment transport on streambed clogging. *Hydrological Processes*, 19(2), 413–427. https://doi.org/10.1002/hyp.5540
- Ren, J., & Packman, A. I. (2002). Effects of background water composition on stream-subsurface exchange of submicron colloids. *Journal of Environmental Engineering*, 128(7), 624–634. https://doi.org/10.1061/(asce)0733-9372(2002)128:7(624)
- Song, J., Chen, X., Cheng, C., Summerside, S., & Wen, F. (2007). Effects of hyporheic processes on streambed vertical hydraulic conductivity in three rivers of Nebraska. *Geophysical Research Letters*, 34(7). https://doi.org/10.1029/2007gl029254
- Song, J., Wang, L., Dou, X., Wang, F., Guo, H., Zhang, J., et al. (2018). Spatial and depth variability of streambed vertical hydraulic conductivity under the regional flow regimes. *Hydrological Processes*, 32(19), 3006–3018. https://doi.org/10.1002/hyp.13241
- Syvitski, J. P. M., Peckham, S. D., Hilberman, R., & Mulder, T. (2003). Predicting the terrestrial flux of sediment to the global ocean: A planetary perspective. *Sedimentary Geology*, 162(1–2), 5–24. https://doi.org/10.1016/s0037-0738(03)00232-x
- Tiegs, S. D., Costello, D. M., Isken, M. W., Woodward, G., McIntyre, P. B., Gessner, M. O., et al. (2019). Global patterns and drivers of ecosystem functioning in rivers and riparian zones. Science Advances, 5(1), 1–9. https://doi.org/10.1126/sciadv.aav0486
- Tonina, D., Luce, C., & Gariglio, F. (2014). Quantifying streambed deposition and scour from stream and hyporheic water temperature time series. Water Resources Research, 50(1), 287–292. https://doi.org/10.1002/2013wr014567
- Trauth, N., Schmidt, C., Vieweg, M., Oswald, S. E., & Fleckenstein, J. H. (2015). Hydraulic controls of in-stream gravel bar hyporheic exchange and reactions. *Water Resources Research*, 51(4), 2243–2263. https://doi.org/10.1002/2014wr015857

TEITELBAUM ET AL. 12 of 13





- Voepel, H., Schumer, R., & Hassan, M. A. (2013). Sediment residence time distributions: Theory and application from bed elevation measurements. *Journal of Geophysical Research: Earth Surface*, 118(4), 2557–2567. https://doi.org/10.1002/jgrf.20151
- Wharton, G., Mohajeri, S. H., & Righetti, M. (2017). The pernicious problem of streambed colmation: A multi-disciplinary reflection on the mechanisms, causes, impacts, and management challenges. WIREs Water, 4, e1231. https://doi.org/10.1002/wat2.1231
- Wohl, E. (2015). Legacy effects on sediments in river corridors. Earth-Science Reviews, 147, 30-53. https://doi.org/10.1016/j.earscirev.2015.05.001
- Wolke, P., Teitelbaum, Y., Deng, C., Lewandowski, J., & Arnon, S. (2020). Impact of bed form celerity on oxygen dynamics in the hyporheic zone. Water, 12(1), 5–7. https://doi.org/10.3390/w12010062
- $Wolman, M. G. (1967). \ A cycle of sedimentation and erosion in Urban River channels. \textit{Geografiska Annaler: Series A, Physical Geography, } 49(2), 385-395. \ https://doi.org/10.1080/04353676.1967.11879766$
- Wood, P. J., & Armitage, P. D. (1997). Biological effects of fine sediment in the lotic environment. *Environmental Management*, 21(2), 203–217. https://doi.org/10.1007/s002679900019
- Wu, G., Shu, L., Lu, C., Chen, X., Zhang, X., Appiah-Adjei, E. K., & Zhu, J. (2015). Variations of streambed vertical hydraulic conductivity before and after a flood season. *Hydrogeology Journal*, 23(7), 1603–1615. https://doi.org/10.1007/s10040-015-1275-9
- Zheng, L., Cardenas, M. B., Wang, L., & Mohrig, D. (2019). Ripple effects: Bed form morphodynamics cascading into hyporheic zone biogeochemistry. Water Resources Research, 55(8), 7320–7342. https://doi.org/10.1029/2018wr023517

TEITELBAUM ET AL. 13 of 13